

Determination of the pK for the Acid-Induced Denaturation of Ferrocycytochrome *c*<sup>†</sup>Rastislav Varhač<sup>§</sup> and Marián Antalík<sup>\*,§,‡</sup>

Department of Biophysics, Institute of Experimental Physics, Slovak Academy of Sciences,  
Watsonova 47, 043 53 Košice, Slovakia, and Department of Biochemistry, Faculty of Sciences,  
P. J. Šafárik University, Moyzesova 11, 041 54 Košice, Slovakia

Received November 11, 2003; Revised Manuscript Received January 28, 2004

**ABSTRACT:** Optical absorption spectroscopy was used to characterize the acid-induced conformational transition of horse heart ferrocycytochrome *c* in the presence of urea. By using linear extrapolation to zero denaturant concentration, an apparent pK value for denaturation was found to be  $0.86 \pm 0.07$  at 25 °C. Visible absorption spectra in the presence of high urea concentration indicate that the dominant population is a high-spin, five-coordinate form under acidic conditions. Ferricytochrome *c*, used as a model reference system, shows a linear dependence of pK values versus urea concentration in the range from 0 to 4.1 M. Our data also indicate that even at a pH below 2 the iron–sulfur bond in ferrocycytochrome *c* is present.

It has been known for a long time that there is a striking difference between ferrocycytochrome *c* (ferrocyt *c*)<sup>1</sup> and ferricytochrome *c* (ferricyt *c*) in the resistance toward denaturation and external-ligand binding (1–7). In ferrocyt *c*, the bond between the sulfur of Met80 and iron and the polypeptide fold are stable over a wide range of temperatures, concentration of denaturant, and pH. For example, the transition temperature ( $T_m$ ) for the cleavage of the iron–sulfur bond of oxidized cytochrome *c* (cyt *c*) at neutral pH is observed at 57.4 °C and precedes the global unfolding at 85.4 °C (8–12). However, for reduced cyt *c* there is a  $T_m$  of 100.6 °C that is thought to correspond to both cleavage of the Fe–S bond and the overall unfolding (13). Similarly, the concentration ( $C_m$ ) of guanidine hydrochloride (GdnHCl) that causes 50% unfolding for reduced cyt *c* (~5 M) is twice as high as that for oxidized cyt *c* (~2.5 M) (7, 14–17). The same is true for the sensitivity of cyt *c* to pH. Earlier experiments have shown that ferrocyt *c* maintains its native absorption profile at pH values which were found to cause a rupture of the Fe–S bond in ferricyt *c* (18–21). Altogether these results reveal that the free energies of unfolding ( $\Delta G_D$ ) for oxidized and reduced cyt *c* differ by 30–40 kJ mol<sup>−1</sup> at neutral pH (7, 14–16, 22, 23).

The remarkably high stability of the reduced form originates from two main sources. One is the strengthening of the Fe–S(Met80) bond as a consequence of metal-to-ligand  $\pi$ -back-bonding in going from the ferric to the ferrous state (24, 25). For comparison, at 25 °C and pH 7.5 the strength of the Fe–S bond expressed in terms of free energy has been estimated to be 14.6 and 8.4 kJ mol<sup>−1</sup> for ferrous and ferric cyt *c*, respectively (26). The second contribution

comes from the zero net charge on ferrocyt *c* heme iron, which is more favorable in the hydrophobic interior of the protein than the destabilizing positively charged ferricyt *c* heme (22, 23).

The pH transitions of mitochondrial ferricyt *c* between pH 2 and pH 11 were determined a long time ago (27). However, similar data are missing for ferrocyt *c*. With both acidic and alkaline transitions that are directly related to breaking of the Fe–S bond, only the pK of the alkaline transition has been determined by indirect electrochemical experiments (28, 29). To our knowledge, the pK value of the acidic transition for ferrocyt *c* has yet to be established. Most efforts have failed because of a lack of an efficient reducing agent (19), precipitation of the sample (18), or a rapid oxidation of the unfolded ferrocyt *c* (30). In addition, for the very low acidic transition, a difficulty associated with acid-induced molten globule state formation (31) may be expected to complicate measurements. These issues can be overcome by using urea that shifts the acidic pK of cyt *c* to higher values (11, 32).

In an effort to provide the missing information, we have performed acid-induced denaturation of ferrocyt *c* at variable concentrations of urea. The acidic pK for horse heart ferrocyt *c* was determined by means of linear extrapolation to zero urea concentration.

## MATERIALS AND METHODS

Horse heart cyt *c* (type VI, Sigma) was used without further purification. Sodium dithionite (Na<sub>2</sub>S<sub>2</sub>O<sub>4</sub>) was obtained from Sigma and potassium ferricyanide (K<sub>3</sub>[Fe(CN)<sub>6</sub>]) was from Aldrich. Urea (Aldrich) solutions were freshly prepared in 5 mM sodium phosphate (Lachema, Czech Republic) and used within 1 day. Precise urea concentrations were determined by refractive index measurements (Abbe refractometer, CETI, Belgium) (33).

**Absorption Measurements.** Absorption measurements were made with a Shimadzu UV-3000 spectrophotometer. Cuvettes were thermostated by water circulation and the temperature was read using a thermometer immersed in the

<sup>†</sup> This work was supported by the Slovak Grant Agency (Grant No. 3198).

\* To whom correspondence should be addressed. Tel.: +421-55-6782240. Fax: +421-55-6783754. E-mail: antalik@saske.sk.

<sup>§</sup> Slovak Academy of Sciences.

<sup>‡</sup> P. J. Šafárik University.

<sup>1</sup> Abbreviations: cyt *c*, cytochrome *c*; ferricyt *c*, ferricytochrome *c*; ferrocyt *c*, ferrocycytochrome *c*; GdnHCl, guanidine hydrochloride; NMR, nuclear magnetic resonance.

reference cuvette. All titrations were performed at  $25.0 \pm 0.3$  °C.

**pH Measurements and Corrections.** pH was determined using a HI 9017 pH meter coupled to a HI 1330 pH electrode (Hanna Instruments Srl, Italy). The pH-correction terms ( $\delta\text{pH}^*$ ) for urea solutions were implemented according to Acevedo et al. (34).

**pH Titrations of Ferricyt *c*.** The pH of the cyt *c* solution was gradually adjusted by addition of small amounts of concentrated HCl (Lachema). The protein was fully oxidized by addition of  $1\ \mu\text{L}$  of  $10\ \text{mM}\ \text{K}_3[\text{Fe}(\text{CN})_6]$  into a  $2500\ \mu\text{L}$  sample volume. The absorbance at  $394\ \text{nm}$  ( $A_{394}$ ) was monitored and used to plot  $A_{394}$  versus pH at the various urea concentrations. Ferricyt *c* concentration ( $4.5 \pm 0.1\ \mu\text{M}$ , the error was calculated as the standard deviation of multiple determinations) was determined spectrophotometrically by using an extinction coefficient at  $410\ \text{nm}$ ,  $\epsilon_{410} = 106\ \text{mM}^{-1}\ \text{cm}^{-1}$  (35).

**pH Titrations of Ferrocyc *c*.** Prior to reduction, the cyt *c* solution ( $2200\ \mu\text{L}$ ; pH adjusted with concentrated HCl) was deoxygenated with argon (Messer Tatragas, Slovakia) for 10–15 min. The gas was passed through an alkaline pyrogallol solution ( $\sim 5\%$ ) to scavenge oxygen. A total of  $200\text{--}300\ \mu\text{L}$  of reduced stock solution (consisting of urea and cyt *c* of the same concentration as in the cuvette,  $5\ \text{mM}$  phosphate,  $100\ \text{mM}\ \text{Na}_2\text{S}_2\text{O}_4$ ) was then added into the cuvette through a needle in the stopper. A brief bubbling with argon was used to mix the solutions, and the absorbance at  $424\ \text{nm}$  was recorded within 10 s after addition of the reducing solution. The precise pH was determined after each recording of the absorbance, and new protein sample at a different pH value was then prepared. In some experiments, a pH jump was used to acquire relevant data. A deoxygenated protein solution was reduced by solid sodium dithionite, the pH was adjusted to  $\sim 6.5$ , and a small amount of concentrated HCl was used to acidify the solution. The precise pH was measured after recording the absorbance. The concentration of ferrocyc *c* ( $5.2 \pm 0.1\ \mu\text{M}$ ) was determined using an extinction coefficient of  $28\ \text{mM}^{-1}\ \text{cm}^{-1}$  at  $550\ \text{nm}$  (35).

**Analysis of the Titration Curves.** Data were analyzed as a single-step process ( $\text{N} \rightleftharpoons \text{U}$ ) applying a nonlinear least-squares fit according to the following equation:

$$A_{\text{obs}} = \frac{A_{\text{N}} + A_{\text{U}}10^{n(\text{pK}-\text{pH})}}{1 + 10^{n(\text{pK}-\text{pH})}} \quad (1)$$

where  $A_{\text{obs}}$  is the observed absorbance at  $394$  and  $424\ \text{nm}$  for ferricyt *c* and ferrocyc *c*, respectively,  $A_{\text{N}}$  and  $A_{\text{U}}$  are absorbances of native and unfolded forms, respectively,  $n$  is the number of protons involved in the transition, and  $\text{pK}$  is the midpoint of the transition.

## RESULTS

Using optical absorption spectroscopy, the acid-induced unfolding of ferric and ferrous cyt *c* was monitored in the presence of various urea concentrations. The convenience of this technique is in the direct characterization of denaturant species with respect to axial ligand configuration. The Soret band absorption was used as a probe sensitive both to heme ligation and the spin state of the heme iron. To compare the absorption changes accompanying unfolding of ferric and

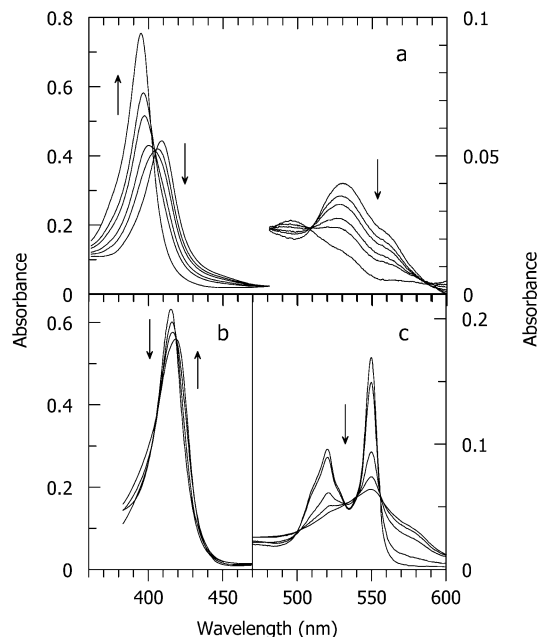


FIGURE 1: Absorption spectra of (a) ferricyt *c* in  $2.9\ \text{M}$  urea at pH 6.45, 3.75, 3.68, 3.60, 3.54, 2.36, and ferrocyc *c* in  $9.0\ \text{M}$  urea; (b) pH 6.88, 5.05, 4.76, 4.55; and (c) 6.85, 5.10, 4.77, 4.59, 4.54;  $5\ \text{mM}$  sodium phosphate,  $25\ ^\circ\text{C}$ . Up and down arrows indicate an increase and a decrease in absorbance with decreasing pH, respectively.

ferrous cyt *c* by urea, the absorption profiles of the former in  $2.9\ \text{M}$  urea and the latter in  $9.0\ \text{M}$  urea were performed at several pH values (Figure 1). The fundamental difference between these two is in the opposite shifts of the Soret band as the acid concentration increases. This makes the Soret band an unambiguous probe for the detection of unfolded individual redox forms. Decreasing the pH induces a blue shift of the ferricyt *c* Soret maximum from  $409\ \text{nm}$  (pH 6.45) to  $394\ \text{nm}$  (pH 2.36), indicating the transition of the heme iron from a low- to a high-spin form (Figure 1a) (32, 36). In addition,  $\beta$  peak initially centered at  $530\ \text{nm}$  markedly diminishes and a small band develops at about  $495\ \text{nm}$  in  $2.9\ \text{M}$  urea at acidic pH.

It was shown previously that the presence of high urea concentrations do not change the absorption characteristics of native ferrocyc *c* at neutral pH, specifically the  $\alpha$ ,  $\beta$  and Soret maxima at  $550$ ,  $520.5$ , and  $415\ \text{nm}$ , respectively (Figure 1b,c) (37). By contrast, under acidic conditions a red shift of the Soret band to  $419\ \text{nm}$  is observed for urea-treated ferrocyc *c* (Figure 1b). The concomitant reduction of  $\alpha$ -band intensity and the disappearance of  $\beta$  band are consistent with dissociation of the native Met80 ligand leaving the heme iron five-coordinate (Figure 1c) (13, 38). Lowering the pH also induces a new shoulder at  $\sim 580\ \text{nm}$ , similar to that appearing in the spectra of GdnHCl-treated ferrocyc *c* at high temperatures and neutral pH (13).

The acid-induced unfolding of both redox forms in the absence and presence of urea are shown in Figure 2. All transition profiles exhibit the sigmoidal shape expected for an apparent two-state process. In the case of oxidized cyt *c*, the absorbance at  $394\ \text{nm}$  as an indicator of a high-spin state of  $\text{Fe}^{3+}$  was recorded (Figure 2a). Data were analyzed applying the two-state mechanism (eq 1) that yielded  $\text{pK}$  and  $n$  values presented in Table 1. It should be noted that the upper part of the transition zones (especially between pH 3

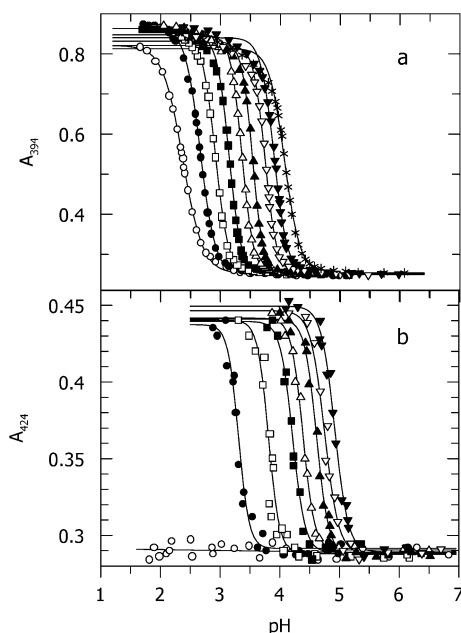


FIGURE 2: Acid titrations of (a) ferricyt *c* in 0 M (○), 0.5 M (●), 1.0 M (□), 1.5 M (■), 2.1 M (△), 2.5 M (▲), 3.1 M (▽), 3.5 M (▼) and 4.1 M (\*) urea monitored at 394 nm, and (b) ferrocyt *c* in 0 M (○), 5.0 M (●), 6.0 M (□), 7.0 M (■), 7.5 M (△), 8.0 M (▲), 8.5 M (▽), and 9.0 M (▼) urea monitored at 424 nm; 5 mM sodium phosphate, 25 °C. The solid curves are nonlinear least-squares fits to eq 1. The symbols represent raw experimental data without pH correction for urea solutions.

Table 1: Parameters from Fit to pH Titrations of Ferricyt *c* in Different Urea Concentrations at 25 °C<sup>a</sup>

urea conc (M)	pK	pK <sup>*b</sup>	n
0	2.38 ± 0.02	2.38	2.6 ± 0.1
0.5	2.66 ± 0.04	2.48	3.5 ± 0.3
1.0	2.91 ± 0.03	2.57	4.1 ± 0.2
1.5	3.14 ± 0.02	2.66	4.3 ± 0.2
2.1	3.36 ± 0.02	2.74	4.5 ± 0.3
2.5	3.53 ± 0.02	2.81	4.7 ± 0.2
3.1	3.74 ± 0.03	2.91	4.4 ± 0.2
3.5	3.89 ± 0.03	2.99	3.8 ± 0.2
4.1	4.07 ± 0.02	3.07	3.4 ± 0.1

<sup>a</sup> The errors in pK and *n* were evaluated as standard deviation from three measurements. <sup>b</sup> pK<sup>\*</sup> values take into consideration pH-correction factors for urea solutions; pK<sup>\*</sup> = pK + δpH\*, where δpH\* is correction factor for corresponding urea concentration (34).

and 4) recorded in urea solutions clearly shows some deviation from the simple two-state model. This deviation is more noticeable in higher urea concentrations and most probably indicates minor conformational process related to heme coordination.

Titration curves for ferrocyt *c* were monitored by following the increase in absorbance at 424 nm upon decreasing the pH (Figure 2b). It should be mentioned here that because of rapid ferrocyt *c* oxidation, especially when unfolded, each symbol represents a measurement on the individual protein sample. The unfolding curves were analyzed assuming the two-state transition between the folded and unfolded states. Both parameters pK and *n* are summarized in Table 2. As can be seen from Figure 2b, no transition of ferrocyt *c* is observed in urea-free medium between pH 1.8 and 6.8.

The unfolding experiments for ferric and ferrous cyt *c* yielded two sets of pK, which were analyzed in more detail (Figure 3). The original data showed a nonlinear dependence

Table 2: Parameters from Fit to pH Titrations of Ferrocyt *c* in Different Urea Concentrations at 25 °C<sup>a</sup>

urea conc (M)	pK	pK <sup>*b</sup>	n
5.0	3.31 ± 0.09	2.16	4.8 ± 1.0
6.0	3.81 ± 0.07	2.50	4.7 ± 0.7
7.0	4.21 ± 0.05	2.76	4.7 ± 0.5
7.5	4.39 ± 0.06	2.86	4.5 ± 0.4
8.0	4.62 ± 0.04	3.03	4.3 ± 0.3
8.5	4.75 ± 0.04	3.12	3.7 ± 0.5
9.0	4.92 ± 0.05	3.25	3.9 ± 0.4

<sup>a</sup> The errors in pK and *n* were evaluated as standard deviation from three measurements. <sup>b</sup> pK<sup>\*</sup> values take into consideration pH-correction factors for urea solutions; pK<sup>\*</sup> = pK + δpH\*, where δpH\* is correction factor for corresponding urea concentration (34).

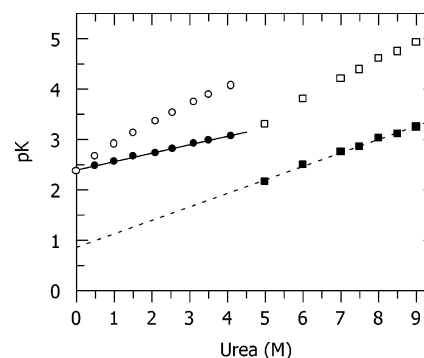


FIGURE 3: Dependence of pK values on urea concentration. The symbols denote pK (○, uncorrected) and pK<sup>\*</sup> (●, corrected for urea concentration) for ferricyt *c*, and pK (□) and pK<sup>\*</sup> (■) for ferrocyt *c*. The straight lines are linear least-squares fits to the following equation: pK = *a* + *b*[urea], where *a* is the pK value at zero denaturant concentration and *b* is the slope of the line. The fitted values are *a* = 2.39 ± 0.01 and 0.86 ± 0.07 for ferricyt *c* and ferrocyt *c*, respectively, and *b* = 0.17 ± 0.01 and 0.27 ± 0.01 M<sup>-1</sup> for ferricyt *c* and ferrocyt *c*, respectively. The errors in the slopes and intercepts are obtained from the fitting.

of pK upon pH that disappeared after introducing a pH correction for urea concentrations (34). For ferricyt *c*, the corrected pK values (pK<sup>\*</sup>) yield an intercept of 2.39 ± 0.01 for the linear fit. This is in agreement with experimental value of 2.38 ± 0.02 (Table 1). For ferrocyt *c*, applying a linear extrapolation to zero urea concentration, pK<sup>\*</sup> values yielded a pK of 0.86 ± 0.07. This finding is in accord with our observation of no transition down to pH of 1.8 in urea-free medium (Figure 2b). The slopes of these fits were found to be 0.17 ± 0.01 and 0.27 ± 0.01 M<sup>-1</sup> for ferricyt *c* and ferrocyt *c*, respectively.

## DISCUSSION

It has been demonstrated that ferricyt *c* undergoes four conformational transitions as the pH is raised from 0 to 14 (27). The so-called state III of ferricyt *c* (27) has His18 and Met80 in their positions as fifth and sixth axial ligands to the heme iron (39, 40); this is the form that functions as an electron carrier in mitochondria. Upon acidification, the protein undergoes conversion from state III to state II accompanied by a change in heme iron from a low-spin state to a high-spin state with a water molecule replacing Met80; the apparent pK for the III → II transition is around 2.5 (36, 41–44). The III → IV alkaline transition proceeds with a pK in the range of 8–11, depending on the source of ferricyt *c* (45).



Until now only a single, alkaline transition has been determined for ferrocycyt *c*, by an indirect electrochemical procedure. The  $pK$  values were found to be 16.8, 16.3, and 14.4 for horse, yeast, and beef ferrocycyt *c*, respectively (28, 29). Low flexibility, high compactness, a different level of hydration, and an almost 2-fold increase in the affinity of sulfur for iron in ferrocycyt *c* relative to ferricyct *c* increase the stability and reduce the unfolding of the former at conventional pH values. In the present experiments, we show that ferrocycyt *c* that has been destabilized by the presence of an appropriate denaturant could be conveniently acid-unfolded.

The most probable model describing the acid-induced transition of ferrocycyt *c* seems to be the one representing a transition from the native, low-spin form to a high-spin form. The absorption spectrum of ferrocycyt *c* in 9.0 M urea at low pH strongly suggests that its unfolded form adopts high-spin configuration with His18 serving as the only axial ligand. This argument is supported by the similarity of the visible spectrum with that of five-coordinate reduced species and models (21, 40, 46, 47). This is in contrast to observations on the isothermal unfolding of ferrocycyt *c* induced by GdnHCl at neutral pH and room temperature with bis-His heme coordination in the unfolded state (15, 38). However, the bis-His configuration of ferrocycyt *c* can be readily disrupted by elevated temperatures (13) or by decreasing the pH (38). Moreover, the observation of a single-step transition from the native low-spin heme directly to the high-spin heme can be accomplished using the anionic detergent sodium dodecyl sulfate (SDS) at room temperature and near neutral pH (21).

The acid-induced transitions of ferricyct *c* show three characteristics (Figure 2a). First, an increase of urea concentration shifts the  $pK$  to higher values as was already demonstrated for the denaturant-treated protein (11, 48). Second, the absorbance of denatured ferricyct *c* at 394 nm is smaller in the absence of urea than in its presence. In the absence of urea, the lower pH and associated higher concentration of HCl is required to complete the transition compared to the transitions in the presence of urea. Consequently, without urea the screening of the positively charged groups of the protein is more effective due to the higher chloride ions (31), and the denatured protein is in a more compact state. In the presence of urea, the transition occurs at lower HCl concentration, which in turn brings about less effective screening with the more expanded denatured state of the protein. We suggest that the differences in the expansion of denatured states are the reason for the differences in the intensity absorption at 394 nm below pH 2. Third, there is a deviation from the regular sigmoidal transition for the urea-treated ferricyct *c*. Transitions in the presence of urea are the most probably the result of two consecutive processes. The most important is the transition from the native form (His18/Met80) directly to the denatured form (His18/H<sub>2</sub>O) as was mentioned above for urea-free solutions. However, there is a minor process, occurring at the presence of urea that we ascribe to the transition from the native state to the bis-His intermediate followed by the transition to the final His18/H<sub>2</sub>O species. However, we have not observed this kind of behavior for ferrocycyt *c* unfolding.

We have exploited varying the urea concentration to shift the acid-induced transition of ferricyct *c* to higher pH. We found that the dependence of  $pK$  for acid denaturation on

urea concentration is linear. However, the initial state of ferricyct *c*, at any of the urea concentrations employed, can be reliably ascribed to the native His18/Met80 species. As published data show, the native state of ferricyct *c* can be guaranteed up to ~4 M of urea. For example, an NMR study demonstrated that more than 85% of ferricyct *c* is in its native state up to 5 M urea at neutral pH (49). Similar results were also obtained using tryptophan fluorescence, absorption spectroscopy, and circular dichroism (11, 17). Further increases in urea concentration above 5 M cause disruption of the Fe–S(Met80) bond and substitution of methionine for another strong-field ligand, histidine (10, 50). In addition, small amounts of His18/Lys derivatives of ferricyct *c* were found to be present in low urea concentrations (<5 M) at neutral pH (49).

On the other hand, for ferrocycyt *c* at and near neutral pH there is no urea-inducing conformational change. However, there is a serious limitation associated with acid-induced transition of ferrocycyt *c* in the presence of urea. It arises from a dramatic decrease in the reduction potential of cyt *c* from +286 to –0.167 mV (versus the normal hydrogen electrode) upon unfolding (14). In the unfolded state, reduced heme becomes more easily oxidized, and acidification of the solution accelerates this process. In addition, one of the most efficient reduction agents, sodium dithionite, if used in excess, produces turbidity at low pH values. For these reasons, a greater extrapolation to zero urea concentration was needed to obtain the apparent  $pK$  for the acid-unfolding ferrocycyt *c* than was necessary with ferricyct *c*.

According to Fink et al. (51), there are 2–4 protons involved in the acid-induced unfolding of type I proteins including ferricyct *c*. Our findings of 2.6 protons (Table 1) are in a good agreement with this classification. The participation of approximately three protons in the acid-induced transition of ferricyct *c* is also confirmed by the results of other authors using the Soret absorbance as a probe (41, 52, 53). This number is increased to 4.7 in the presence of 2.5 M urea. Comparable  $n$  values (3.9–4.8) were achieved using ferrocycyt *c* (Table 2), although only in the presence of 5.0–9.0 M urea. The dependence of  $n$  on denaturant concentration in the ranges studied is not linear. The enhancement of  $n$  by 1–2 units upon urea addition implies a more complex behavior relative to urea-free cyt *c*. This observation is in contrast to single proton-associated transitions in the presence of anions. However, anions were shown to simplify the unfolding reactions (52). The different mode of action of these two agents is explained by urea stabilization of the unfolded state relative to the folded state, and tendency of salts to stabilize the intermediate state with retained secondary structure elements.

To further follow the classification of Fink et al. (51), ferrocycyt *c* belongs to type III class with no transition down to pH 1. The notable decrease in the  $pK$  upon reduction of cyt *c* reflects the extra stabilization of the native state by intrinsic forces. It is reasonable to assume that difference in  $pK$  values for ferricyct *c* and ferrocycyt *c* results from the difference in  $\Delta G_D$  of these two oxidation states. To quantify this difference through the  $pK$  values, we have used the equation  $\Delta\Delta G_{\text{red-ox}} = 2.303RTn\Delta pK$  (54), where  $R$  is the gas constant,  $T$  is absolute temperature (298 K),  $n$  is the number of protons involved in the unfolding of urea-free cyt *c*, and  $\Delta pK$  is the difference in transition midpoints

between ferricyt *c* (2.38) and ferrocyt *c* (0.86). As mentioned above, the acid-induced unfolding of cyt *c* is a process involving  $\sim 3$  protons in the absence of urea. If we assume that the number of titratable sites responsible for the unfolding transition is independent of the redox state of cyt *c*, then the above equation gives a value of  $\Delta\Delta G_{\text{red-ox}}$  of  $26.0 \text{ kJ mol}^{-1}$ . Earlier equilibrium measurements performed at neutral pH revealed the difference in unfolding free energies of ferricyt *c* and ferrocyt *c* ranging from 30 to 40  $\text{kJ mol}^{-1}$  (at 10–40 °C) (7, 14–16). Our value varies by about 4–14  $\text{kJ mol}^{-1}$ , which implies an involvement of more than three protons in acid-induced transition of cyt *c* and, of course, this is the case in the presence of urea.

In this study, we have characterized the acid-induced conformational transition of horse heart ferrocyt *c* in the presence of urea. By using a linear extrapolation to zero denaturant concentration, an apparent  $pK$  value for horse heart ferrocyt *c* unfolding was found to be  $0.86 \pm 0.07$  at 25 °C. A particular advantage of this approach is that the  $pK$  values measured in urea solutions are not affected by the presence of the molten globule state.

## ACKNOWLEDGMENT

We thank Dr. Marián Fabian and Professor Graham Palmer for helpful comments on the manuscript.

## REFERENCES

- Butt, W. D., and Keilin D. (1962) Absorption spectra and some other properties of cytochrome *c* and of its compounds with ligands. *Proc. R. Soc. London Ser. B* 156, 429–458.
- George, P., and Schejter, A. (1964) The reactivity of ferrocytochrome *c* with iron-binding ligands. *J. Biol. Chem.* 239, 1504–1508.
- Moore, T. A., Greenwood, C., and Wilson, M. T. (1975) Ligand binding to ferrocytochrome *c* at high pH. *Biochem. J.* 147, 335–341.
- Moore, G. R., and Williams, R. J. (1980) Nuclear-magnetic-resonance studies of ferrocytochrome *c*. pH and temperature dependence. *Eur. J. Biochem.* 103, 513–521.
- Yu, C. A., Steidl, J. R., and Yu, L. (1983) Microcalorimetric studies of the interactions between cytochromes *c* and *c*<sub>1</sub> and of their interactions with phospholipids. *Biochim. Biophys. Acta* 736, 226–234.
- Hilgen-Willis, S., Bowden, E. F., and Pielak, G. J. (1993) Dramatic stabilization of ferrocytochrome *c* upon reduction. *J. Inorg. Biochem.* 51, 649–653.
- Pascher, T., Chesick, J. P., Winkler, J. R., and Gray, H. B. (1996) Protein folding triggered by electron transfer. *Science* 271, 1558–1560.
- Bágel'ová, J., Antalík, M., and Tomori, Z. (1997) Effect of polyglutamate on the thermal stability of ferricytochrome *c*. *Biochem. Mol. Biol. Int.* 43, 891–900.
- Santucci, R., Giartosio, A., and Ascoli, F. (1989) Structural transitions of carboxymethylated cytochrome *c*: calorimetric and circular dichroic studies. *Arch. Biochem. Biophys.* 275, 496–504.
- Myer, Y. P. (1968) Conformation of cytochromes. III. Effect of urea, temperature, extrinsic ligands, and pH variation on the conformation of horse heart ferricytochrome *c*. *Biochemistry* 7, 765–776.
- Myer, Y. P., MacDonald, L. H., Verma, B. C., and Pande, A. (1980) Urea denaturation of horse heart ferricytochrome *c*. Equilibrium studies and characterization of intermediate forms. *Biochemistry* 19, 199–207.
- Hagihara, Y., Tan, Y., and Goto, Y. (1994) Comparison of the conformational stability of the molten globule and native states of horse cytochrome *c*. Effects of acetylation, heat, urea and guanidine-hydrochloride. *J. Mol. Biol.* 237, 336–348.
- Varhač, R., Antalík, M., and Bánó, M. (2004) Effect of temperature and guanidine hydrochloride on ferrocytochrome *c* at neutral pH. *J. Biol. Inorg. Chem.* 9, 12–22.
- Bixler, J., Bakker, G., and McLendon, G. (1992) Electrochemical probes of protein folding. *J. Am. Chem. Soc.* 114, 6938–6939.
- Thomas, Y. G., Goldbeck, R. A., and Kliger, D. S. (2000) Characterization of equilibrium intermediates in denaturant-induced unfolding of ferrous and ferric cytochromes *c* using magnetic circular dichroism, circular dichroism, and optical absorption spectroscopies. *Biopolymers* 57, 29–36.
- Bhuyan, A. K., and Udgaonkar, J. B. (2001) Folding of horse cytochrome *c* in the reduced state. *J. Mol. Biol.* 312, 1135–1160.
- Hamada, D., Kuroda, Y., Kataoka, M., Aimoto, S., Yoshimura, T., and Goto, Y. (1996) Role of heme axial ligands in the conformational stability of the native and molten globule states of horse cytochrome *c*. *J. Mol. Biol.* 256, 172–186.
- Brumer, P., Levine, W. G., and Peisach, J. (1966) Some properties of denatured horse heart cytochrome *c*. *Arch. Biochem. Biophys.* 117, 232–238.
- Kurihara, M., and Sano, S. (1970) Reduction of cytochrome *c* by ferrous ions and ethylenediaminetetraacetic acid in acid solution. *J. Biol. Chem.* 245, 4804–4806.
- Lambeth, D. O., Campbell, K. L., Zand, R., and Palmer, G. (1973) The appearance of transient species of cytochrome *c* upon rapid oxidation or reduction at alkaline pH. *J. Biol. Chem.* 248, 8130–8136.
- Yoshimura, T. (1988) A change in the heme stereochemistry of cytochrome *c* upon addition of sodium dodecyl sulfate: electron paramagnetic resonance and electronic absorption spectral study. *Arch. Biochem. Biophys.* 264, 450–461.
- Churg, A. K., and Warshel, A. (1986) Control of the redox potential of cytochrome *c* and microscopic dielectric effects in proteins. *Biochemistry* 25, 1675–1681.
- Cohen, D. S., and Pielak, G. J. (1995) Entropic stabilization of cytochrome *c* upon reduction. *J. Am. Chem. Soc.* 117, 1675–1677.
- Schejter, A., and Plotkin, B. (1988) The binding characteristics of the cytochrome *c* iron. *Biochem. J.* 255, 353–356.
- Cheng, M.-C., Rich, A. M., Armstrong, R. S., Ellis, P. J., and Lay, P. A. (1999) Determination of iron-ligand bond lengths in ferric and ferrous horse heart cytochrome *c* using multiple-scattering analyses of XAFS data. *Inorg. Chem.* 38, 5703–5708.
- Viola, F., Aime, S., Coletta, M., Desideri, A., Fasano, M., Paoletti, S., Tarricone, C., and Ascenzi, P. (1996) Azide, cyanide, fluoride, imidazole and pyridine binding to ferric and ferrous native horse heart cytochrome *c* and to its carboxymethylated derivative: a comparative study. *J. Inorg. Biochem.* 62, 213–222.
- Theorell, H., and Åkesson, Å. (1941) Studies on cytochrome *c*. II. The optical properties of pure cytochrome *c* and some of its derivatives. *J. Am. Chem. Soc.* 63, 1812–1818.
- Barker, P. D., and Mauk, A. G. (1992) pH-linked conformational regulation of a metalloprotein oxidation-reduction equilibrium: electrochemical analysis of the alkaline form of cytochrome *c*. *J. Am. Chem. Soc.* 114, 3619–3624.
- Battistuzzi, G., Borsari, M., Loschi, L., Martinelli, A., and Sola, M. (1999) Thermodynamics of the alkaline transition of cytochrome *c*. *Biochemistry* 38, 7900–7907.
- McLendon, G., and Smith, M. (1978) Equilibrium and kinetic studies of unfolding of homologous cytochromes *c*. *J. Biol. Chem.* 253, 4004–4008.
- Goto, Y., Calciano, L. J., and Fink, A. L. (1990) Acid-induced folding of proteins. *Proc. Natl. Acad. Sci. U.S.A.* 87, 573–577.
- Tsong, T. Y. (1975) An acid induced conformational transition of denatured cytochrome *c* in urea and guanidine hydrochloride solutions. *Biochemistry* 14, 1542–1547.
- Pace, C. N. (1986) Determination and analysis of urea and guanidine hydrochloride denaturation curves. *Methods Enzymol.* 131, 266–280.
- Acevedo, O., Guzman-Casado, M., Garcia-Mira, M. M., Ibarra-Molero, B., and Sanchez-Ruiz, J. M. (2002) pH corrections in chemical denaturant solutions. *Anal. Biochem.* 306, 158–161.
- Margoliash, E., and Frohwirt, N. (1959) Spectrum of horse-heart cytochrome *c*. *Biochem. J.* 71, 570–572.
- Myer, Y. P., and Saturno, A. F. (1990) Horse heart ferricytochrome *c*: conformation and heme configuration of low ionic strength acidic forms. *J. Protein Chem.* 9, 379–387.
- Stellwagen, E. (1968) The reversible unfolding of horse heart ferricytochrome *c*. *Biochemistry* 7, 2893–2898.
- Telford, J. R., Tezcan, F. A., Gray, H. B., and Winkler, J. R. (1999) Role of ligand substitution in ferrocytochrome *c* folding. *Biochemistry* 38, 1944–1949.

39. Dickerson, R. E., Takano, T., Eisenberg, D., Kallai, O. B., Samson, L., Cooper, A., and Margoliash, E. (1971) Ferricytochrome *c*. I. General features of the horse and bonito proteins at 2.8 Å resolution. *J. Biol. Chem.* 246, 1511–1535.
40. Harbury, H. A., Cronin, J. R., Fanger, M. W., Hettinger, T. P., Murphy, A. J., Myer, Y. P., and Vinogradov, S. N. (1965) Complex formation between methionine and a heme peptide from cytochrome *c*. *Proc. Natl. Acad. Sci. U.S.A.* 54, 1658–1664.
41. Babul, J., and Stellwagen, E. (1972) Participation of the protein ligands in the folding of cytochrome *c*. *Biochemistry* 11, 1195–1200.
42. Lanir, A., Yu, N. T., and Felton, R. H. (1979) Conformational transitions and vibronic couplings in acid ferricytochrome *c*: a resonance Raman study. *Biochemistry* 18, 1656–1660.
43. Dyson, H. J., and Beattie, J. K. (1982) Spin state and unfolding equilibria of ferricytochrome *c* in acidic solutions. *J. Biol. Chem.* 257, 2267–2273.
44. Oellerich, S., Wackerbarth, H., and Hildebrandt, P. (2002) Spectroscopic characterization of nonnative conformational states of cytochrome *c*. *J. Phys. Chem. B* 106, 6566–6580.
45. Moore, G. R., and Pettigrew, G. W. (1990) *Cytochromes c: Evolutionary, Structural and Physicochemical Aspects*, Springer-Verlag, Berlin.
46. Corradin, G., and Harbury, H. A. (1971) Reconstitution of horse heart cytochrome *c*: interaction of the components obtained upon cleavage of the peptide bond following methionine residue 65. *Proc. Natl. Acad. Sci. U.S.A.* 68, 3036–3039.
47. Yoshimura, T., Fujii, S., Kamada, H., Yamaguchi, K., Suzuki, S., Shidara, S., and Takakuwa, S. (1996) Spectroscopic characterization of nitrosylheme in nitric oxide complexes of ferric and ferrous cytochrome *c* from photosynthetic bacteria, *Biochim. Biophys. Acta* 1292, 39–46.
48. Ibarra-Molero, B., Loladze, V. V., Makhadze, G. I., and Sanchez-Ruiz, J. M. (1999) Thermal versus guanidine-induced unfolding of ubiquitin. An analysis in terms of the contributions from charge–charge interactions to protein stability. *Biochemistry* 38, 8138–8149.
49. Russell, B. S., Melenkivitz, R., and Bren, K. L. (2000) NMR investigation of ferricytochrome *c* unfolding: detection of an equilibrium unfolding intermediate and residual structure in the denatured state. *Proc. Natl. Acad. Sci. U.S.A.* 97, 8312–8317.
50. Muthukrishnan, K., and Nall, B. T. (1991) Effective concentrations of amino acid side chains in an unfolded protein. *Biochemistry* 30, 4706–4710.
51. Fink, A. L., Calciano, L. J., Goto, Y., Kurotsu, T., and Palleros, D. R. (1994) Classification of acid denaturation of proteins: intermediates and unfolded states. *Biochemistry* 33, 12504–12511.
52. Myer, Y. P., and Saturno, A. F. (1991) Horse heart ferricytochrome *c*: conformation and heme configuration of high ionic strength acidic forms. *J. Protein Chem.* 10, 481–494.
53. Sedláč, E., and Antalík, M. (2002) Effect of polyanion on the acidic conformational transition of native and denatured ferricytochrome *c*. Circular dichroism study. *Gen. Physiol. Biophys.* 21, 175–188.
54. Godbole, S., and Bowler, B. E. (1997) A histidine variant of yeast iso-1-cytochrome *c* that strongly affects the energetics of the denatured state. *J. Mol. Biol.* 268, 816–821.

BI036011X